Available online at www.sciencedirect.com
ScienceDirect
Journal of the European Ceramic Society 28 (2008) 1641–1647
www.elsevier.com/locate/jeurceramsoc

Preparation and properties of neodymium-modified bismuth titanate ceramics

Yan-Mei Kan [a], Guo-Jun Zhang [a], Pei-Ling Wang [a,*], Yi-Bing Cheng [b]

[a] *The State Key Lab on High Performance Ceramics and Superfine Microstructure, Shanghai Institute of Ceramics, Chinese Academy of Sciences, Shanghai 200050, China*
[b] *School of Physics and Materials Engineering, Monash University Clayton, Victoria 3168, Australia*

Received 7 July 2007; received in revised form 26 September 2007; accepted 7 October 2007
Available online 4 March 2008

Abstract

Neodymium-modified bismuth titanate (BNT) powder with compositions of $Bi_{4-x}Nd_xTi_3O_{12}$ ($x = 0$, 0.2, 0.5 and 0.75) were prepared through a hydrolysis method. The influence of Nd addition on the powder characteristics, sintering, microstructure and properties were investigated. It was found that the absorption band of Ti–O stretching vibration at 589 cm^{-1} was shifted to a higher wave number in the IR spectra, and the sintering as well as grain growth was significantly retarded. The Curie temperature, dielectric loss and Curie peak intensity were steadily decreased with an increase in Nd concentration, and the dielectric constant and loss tangent became much less dependent on temperature and frequency. At the same time, the polarization properties of the material were greatly improved.

Keywords: $Bi_4Ti_3O_{12}$; Powders-chemical preparation; Sintering; Microstructure-final; Electrical properties

1. Introduction

Bismuth titanate ($Bi_4Ti_3O_{12}$) belongs to the family of Aurivillius layer-structured compounds. As a ferroelectric material, $Bi_4Ti_3O_{12}$ (BIT) has attracted a great deal of attention during recent years. It is thought to be a promising candidate for lead-free ferroelectric oxides, using as nonvolatile random access memories (NvRAMs), high temperature piezoelectric devices and optical displays.[1–4] The crystal structure of $Bi_4Ti_3O_{12}$ is composed of perovskite-like $Bi_2Ti_3O_{10}$ layer alternating with $Bi_2O_2^{2+}$ layers.[5] Due to the formation of vacancy defects in the perovskite blocks, a high dielectric loss and large leakage current are usually observed in $Bi_4Ti_3O_{12}$, which poses an obstacle to the application of BIT in many fields. In order to solve the problem, many researches have been carried out to suppress the conductivity of BIT. Rare earth ions and ions with a higher valence than Ti^{4+} are often used to partially substitute Bi^{3+} and Ti^{4+} ions located in the perovskite unites, respectively. It was reported that the doping of donor cations from group V (e.g. Nb^{5+}, Sb^{5+}, Ta^{5+}) and group VI (e.g. W^{6+}) led to a decrease in the conductivity of BIT by three to four orders up to 600 °C, which facilitated both the poling and high temperature application of $Bi_4Ti_3O_{12}$.[6,7] Our previous study on La-modified $Bi_4Ti_3O_{12}$ ceramics revealed that the loss tangent of $Bi_{3.5}La_{0.5}Ti_3O_{12}$ ceramics at 1 MHz was 8–10 times lower than that of pure BIT ceramics.[8] But there was no obvious improvement of polarization. Recently, Nd-doped $Bi_4Ti_3O_{12}$ films have attracted much attention due to their large remnant polarization.[9–12] It is expected the ferroelectric properties be enhanced by the substitution for Bi of Nd in ceramics. Thus, Nd-modified BIT (BNT) ceramics was prepared using the same method reported in our previous La-modified $Bi_4Ti_3O_{12}$ ceramics. The intensively electric properties were carried out in present work.

2. Experimental procedure

BNT powders with compositions of $Bi_{4-x}Nd_xTi_3O_{12}$ ($x = 0$, 0.2, 0.5 and 0.75, denoted as BIT, BNT02, BNT05 and BNT075, respectively) were prepared by a hydrolysis method as reported elsewhere except La_2O_3 was replaced by Nd_2O_3.[8]

* Corresponding author. Tel.: +86 21 52412324; fax: +86 21 52413122.
E-mail address: plwang@sunm.hcnc.ac.cn (P.-L. Wang).

0955-2219/$ – see front matter © 2007 Elsevier Ltd. All rights reserved.
doi:10.1016/j.jeurceramsoc.2007.10.010

Phase assemblages of the powders were characterized by X-ray diffraction (XRD), using a Guinier-Hägg camera with Cu Kα1 (λ = 1.5405981 Å) as the radiation source and Si as the internal standard. The measurement of X-ray films was conduced on a computer-linked line scanner (LS-18) system. The cell dimensions were determined by means of the PIRUM program-based on the Guinier-Hägg film data.[13] Infrared (IR) analysis was carried out on a FTIR spectrophotometer (Bio-Rad FTS-185, Hercules, CA) by the KBr pellet method.

BNT and BIT powders calcined at 750 °C were uniaxially pressed at 50 MPa in a stainless steel die, followed by isostatic pressing at 200 MPa. The compacts were sintered in air at temperature ranging from 900 °C to 1100 °C for 2 h. Bulk densities of the sintered samples were measured by Archimedes method. Their microstructures were observed on the polished and thermally etched surface by scanning electron microscopy (SEM, XL-30-FEG, FEI, The Netherlands). A JEOL JXA-8100 electron probe microanalyzer (EPMA) with a Link INCA energy spectrum analyzer was used to examine the element compositions in the bulk ceramics. Dielectric properties were determined by an impedance analyzer (HP4192A) on platinum sputtered disks with a diameter of 10 mm and thickness of 1 mm at 100 KHz and 1 MHz, respectively. Ferroelectric hysteresis loops were recorded at 160 °C under a maximum applied field of around 130 kV/cm and frequency of 20 Hz (aixACCT TF analyzer 2000, Germany).

3. Results and discussion

3.1. Powder characterization

The as-prepared BNT precursors were amorphous with a particle size of about 10 nm. The XRD patterns of BNT powder calcined at 600 °C shown in Fig. 1 agreed well with the XRD data of a crystalline $Bi_4Ti_3O_{12}$ (JCPDS card 35–795), no other phases were detected in the powder, indicating that Nd^{3+} ions were incorporated into the lattice of $Bi_4Ti_3O_{12}$. Comparing the crystallizing processes of BNT with that of pure BIT precursor, it was found that a small amount of $Bi_2Ti_2O_7$ intermediate phase was formed in the BIT crystallized powder calcined in the temperature range from 500 °C to 600 °C (Ref. [8]), while no such an

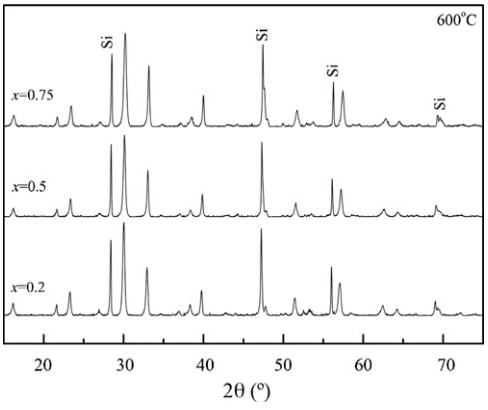

Fig. 1. XRD patterns of $Bi_{4-x}Nd_xTi_3O_{12}$ (x = 0.2, 0.5 and 0.75) powders calcined at 600 °C.

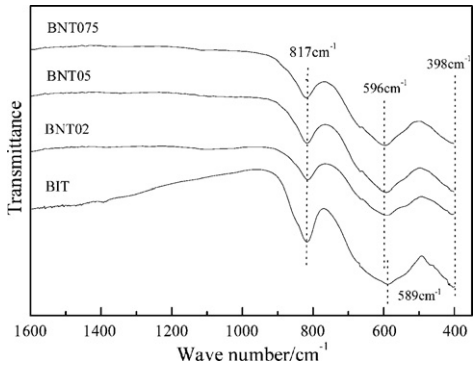

Fig. 2. IR spectra of BIT, BNT02, BNT05 and BNT075 powders.

intermediate phase was observed during the crystallizing process of BNT precursor, revealing that the incorporation of Nd into BIT lattice has suppressed the formation of this intermediate phase.

Fig. 2 shows the IR spectra of BIT and BNT powders calcined at 600 °C. The IR spectrum of BIT was in good agreement with the reported data in previous researches. Three adsorption bands occurring at 817 cm^{-1}, 589 cm^{-1} and 398 cm^{-1} were observed in the IR spectra of BIT. The former two bands could be ascribed to the Ti–O stretching vibrations, while the latter one to the Ti–O bending vibration.[14,15] The IR spectra of BNT powders were similar to that of BIT in general, except the following differences. The adsorption band at 589 cm^{-1} was shifted slightly to a higher wave number of 596 cm^{-1} with increasing Nd doping level, meanwhile the intensity of the band at 817 cm^{-1} was decreased. It is generally recognized that Nd^{3+} often replaces Bi^{3+} ions neighboring the Ti–O octahedrons in the perovskite layer of $Bi_4Ti_3O_{12}$ as x-value less than 1.0.[16] Due to the differences in electronic structure and ion radius between Nd^{3+} and Bi^{3+}, the rotation of Ti–O octahedron accompanied with a shift of the octahedron along a-axis is greatly enhanced by changes in the bond length, strength and even bond angle of Ti–O bonds occurred with the substitution of Nd^{3+} for Bi^{3+}, leading to the differences in the IR spectra between BIT and BNT.

3.2. Sintering and microstructure

The BIT powder showed a high sintering activity, and could be sintered to a high density of 98% at 1000 °C, as shown in Fig. 3. In comparison with the BIT ceramics starting from the powder through solid-state reaction, the sintering temperature of the present BIT sample was much lower.[17] The substitution of Nd for Bi in BNT seemed to retard the sintering and resulted in an increase in the sintering temperature. The optimized sintering temperature was 1050 °C for BNT02 and BNT05, and 1100 °C for BNT075, as shown in Fig. 3. Another interesting feature observed in Fig. 3 is that although all the samples showed a decrease in density when the sintering temperature increased beyond the optimal value, the density decrease became much slower for the sample with a higher Nd concentration. In another words, the incorporation of Nd in BIT has led to a broadening in the sintering temperature range of the material. A high relative density up to 99% could be obtained for all the BNT samples.

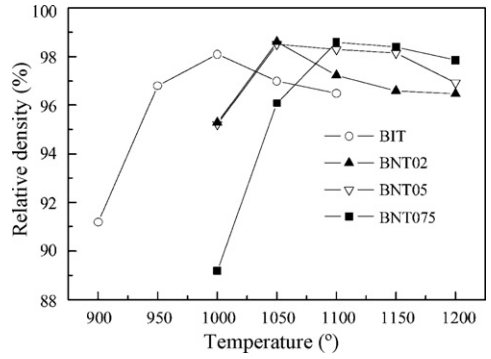

Fig. 3. Densification behavior of BIT, BNT02, BNT05 and BNT075 compacts.

Fig. 4 shows the SEM images of BIT, BNT02 and BNT075 samples sintered at 1050 °C for 2 h. Large rectangular grains of over 10 μm in length were frequently observed in the BIT sample, and the microstructure was very uneven. However with the addition of Nd dopant, a remarkable decrease in the grain size was observed. At the same time, the microstructure also became unprecedentedly uniform. The BNT075 sample showed a mean grain size of only ∼1.5 μm, nearly 5–10 times smaller than that of BIT. In the BNT samples, two kinds of grains could be clearly distinguished according to their difference in contrast and morphology, i.e. dark grey grains with a more equiaxed shape and light grey ones with approximately a rectangular shape. The size of dark grey grains was generally smaller than that of the light grey ones, especially in the sample with low Nd concentration (e.g. BNT02). In order to investigate the difference between these two kinds of grains, XRD and energy-dispersive spectrometer (EDS) measurements were performed on the BNT075 sample. The results of EDS indicated that the dark grey grains contained less Bi and Nd, but more Ti than the light grey ones. The composition of the light grey grains was consistent with that of $Bi_{3.25}Nd_{0.75}Ti_3O_{12}$, while the formula of grains with dark grey color was corresponding to $Bi_{3.10}Nd_{0.55}Ti_{3.27}O_{12}$. Despite the difference in their chemical compositions between the dark and light grey grains, XRD result indicated that there was only one phase in the sample. That is probably because of the low content of dark grey phase in the sample and/or a close similarity between the crystal structures of the two phases.

In accordance with the above findings, it is safe to conclude that the doping of Nd in BIT has greatly influenced the sintering and grain growth of the material as observed in La-modified BIT.[8] An increase in the activating energy for ion migration and reduction in the surface or grain boundary energy were used to explain the increased sintering temperature and reduced grain growth rate in La-modified BIT. This likely holds true in the present case as well, because of the close similarity between Nd^{3+} and La^{3+} ions. Aside from the above reasons, another important factor should be taken into account in the BIT-based system. That is the volatilization of bismuth during sintering at high temperature. The volatilization of bismuth led to formation of bismuth (V_{Bi}''') and oxygen ($V_O^{\bullet\bullet}$) vacancies for charge compensation in the materials, which served as fast mass transport media during sintering. The partial substitution of Nd for Bi has significantly suppressed the volatilization of bismuth in BNT, as deduced from the weight loss values, which are 1.48 wt.%, 0.97 wt.% and 0.49 wt.% for BIT, BNT02 and BNT075 ceramics sintered at 1150 °C for 2 h, respectively, resulting in a decrease in the vacancy concentration and mass transport speed in BNT. Accordingly, the increase in sintering temperature and decrease in grain growth speed in BNT can be well understood.

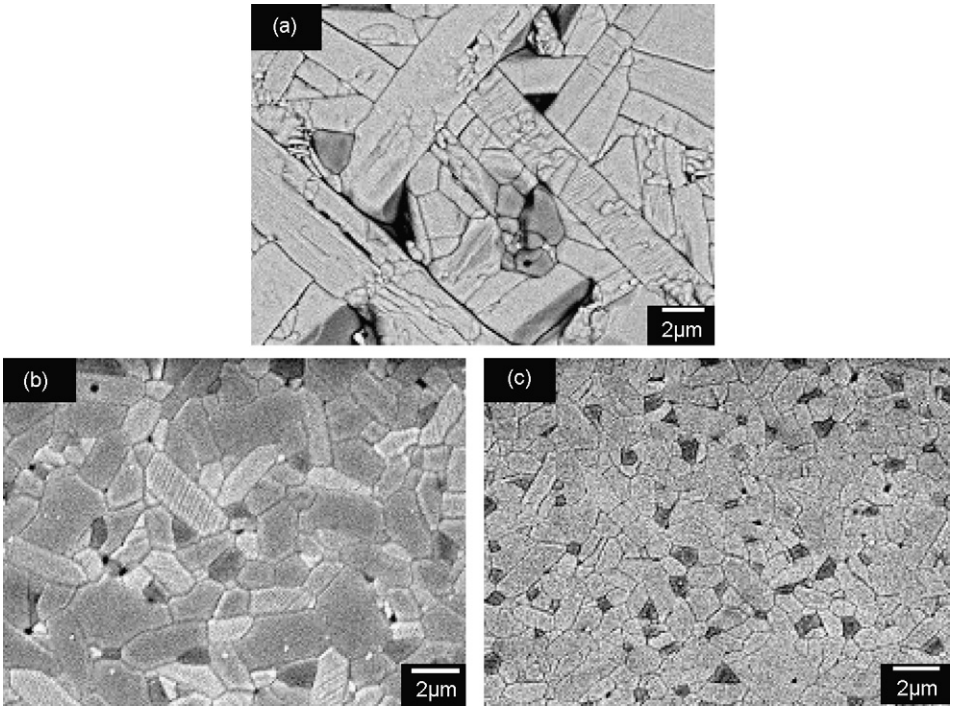

Fig. 4. SEM images of BIT, BNT02 and BBNT075 samples sintered at 1050 °C: (a) BIT; (b) BNT02; (c) BNT075.

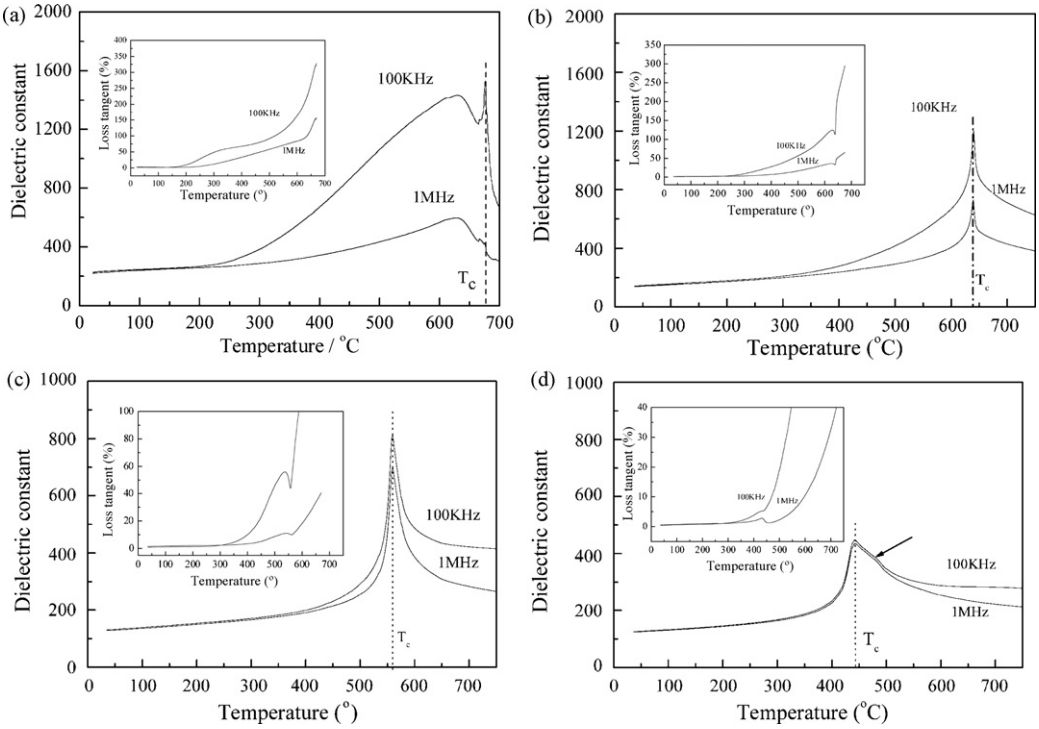

Fig. 5. Dielectric constant and loss tangent of BLT and BIT samples sintered at the respective optimum temperatures: (a) BIT, 1000 °C; (b) BNT02, 1050 °C; (c) BNT05, 1050 °C; (d) BNT075, 1100 °C.

In addition, the dark grey phase, which could be caused by the Bi volatility and deduced of its Ti enrichment, might behave as second phase particles distributed in a matrix of the light grey phase, and thus Zener pinning happened, leading to a microstructure refinement of the material.

3.3. Electric properties

3.3.1. Dielectric property

BIT and BNT samples sintered at their optimum sintering temperatures were used for the measurement of dielectric properties. Fig. 5 shows the temperature dependence of the dielectric constant and loss of BIT and BNT samples measured at 100 KHz and 1 MHz. The BIT sample showed a standard Curie temperature of 675 °C as reported in the literature. While the Curie temperatures of BNT02, BNT05 and BNT075 were 639, 559 °C and 445 °C, respectively. Thus a continuous decrease in the Curie temperature was found with increasing Nd concentration in the BNT samples, which was assumably related to the variation in the crystal structure as discussed below.

Fig. 6 shows parts of the amplified XRD patterns of BIT and BNT powders calcined at 900 °C. Consistent with the JCPDS card for pseudo-orthorhombic $Bi_4Ti_3O_{12}$, the (2 0 0)/(0 2 0) and (2 0 8)/(0 2 8) peaks were well separated into two peaks in the XRD patterns of BIT sample. Other reflections of the BIT with crystallographic index of (*hkl*)/(*khl*) ($h \neq k$), e.g. (2 0 6)/(0 2 6) and (3 1 7)/(1 3 7) also split into two peaks, although they were not shown here. However, these reflection doublets gradually merged into a single peak as Nd^{3+} concentration increased from 0.2 to 0.75, implying a somewhat increase in the symmetry of crystal structure. The lattice parameters of BIT and BNT samples were calculated according to the XRD results and listed in

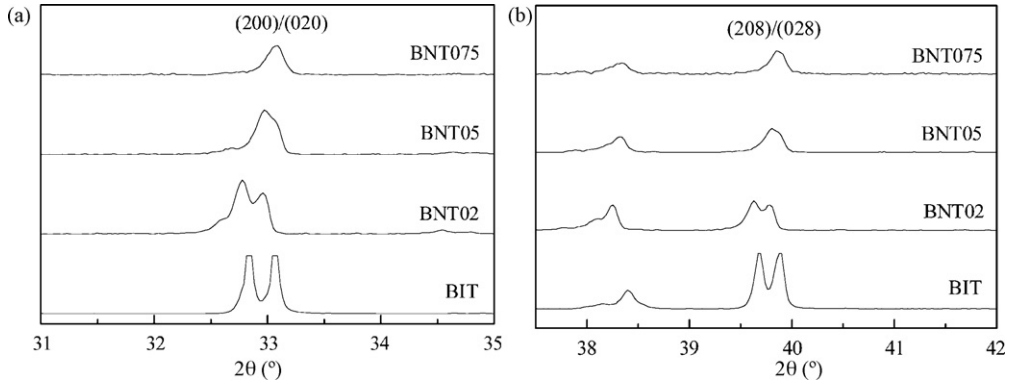

Fig. 6. Parts of the amplified XRD patterns of BIT and BNT powders calcined at 900 °C: (a) (2 0 0)/(0 2 0) peak and (b) (2 0 8)/(0 2 8) peak.

Table 1
Lattice parameters of BIT, BNT02, BNT05 and BNT075

Sample	*a* (Å)	*b* (Å)	*c* (Å)
BIT	5.449 (1)	5.410 (1)	32.82 (1)
BNT02	5.437 (1)	5.407 (1)	32.85 (1)
BNT05	5.418 (1)	5.406 (1)	32.81 (1)
BNT075	5.411 (2)	5.406 (1)	32.85 (1)

Table 1. It can be seen that the lattice constant *a* decreased continuously with increasing Nd concentration, approaching the value of *b*, whereas *b* and *c* remained almost unchanged if the measurement error was taken into account. As a result, the difference between *a* and *b* became increasingly small for the samples with a higher Nd concentration, and the crystal structure symmetry continuously increased. It was the increase in crystal structure symmetry that led to a decrease in the Curie temperature of BNT. The decrease in Curie temperature with an increase in its crystal structure symmetry was well documented in the literature for $BaTiO_3$-based ferroelectrics as well.[18,19] For instance, it was reported that as the *c*/*a* ratio of tetragonal $BaTiO_3$ decreased towards unity with the doping of Sr^{2+}, Sn^{4+} or Zr^{4+}, its Curie temperature was shifted to lower temperature. While in contrast, the substitution of Pb^{2+} for Ba^{2+} in tetragonal $BaTiO_3$ led to an increase in both the *c*/*a* ratio and Curie temperature.

In addition to the variation in Curie temperature, the doping of Nd^{3+} in BIT showed a depressing effect on the Curie peak. In other words, the Curie peak on the dielectric constant curve was broadened with an increase in the Nd^{3+} doping level, and concurrently the Curie peak intensity decreased. The formation of a fine-grained microstructure in BNT might be one of the important reasons accounting for this phenomenon, as observed in $BaTiO_3$ ferroelectrics.[20] Other factors such as an inhomogeneous distribution of Nd^{3+} ions and the formation of secondary phase in BNT could also contribute a lot to the Curie peak depressing, due to the high sensitivity of Curie temperature to chemical compositions. In fact, Curie peak depressing caused by the second phase formation can be distinctively observed for BNT075 sample. On the dielectric curve of BNT075 sample, a shoulder (indicated by an arrow) corresponding to the Curie peak of the secondary phase appeared at 482 °C, which was slightly above the Curie temperature of the matrix (~445 °C), as a result of Nd deficiency in its chemical composition. And the overlapping of the Curie peaks corresponding to the secondary phase and matrix led to the appearance of a broad "Curie peak" of low intensity on the dielectric curve.

The partial substitution of Nd for Bi in BNT resulted in a significant improvement in the dielectric response of the materials as well. The dielectric properties of BIT showed a strong temperature and frequency dependence, because of the existence of strong relaxing polarization processes that were associated with defects formed through the volatilization of bismuth. At a testing frequency of 100KHz, the dielectric constant and loss tangent of BIT increased abruptly above 200 °C, and another peak appeared at ~630 °C on the dielectric curve except the Curie peak. When the testing frequency increased to 1 MHz, the dielectric constant and loss tangent of BIT decreased substantially, as a result of the suppression of relaxing polarization at high frequency. In comparison with BIT, a continuous decrease in the temperature and frequency dependence of dielectric properties was observed for BNT with an increasing Nd concentration, which can be explained by a reduced vacancy concentration in the sample and a smaller contribution of relaxing polarization to its dielectric properties. The dielectric constant and loss tangent curves of BNT became more flattened at a higher Nd doping level, and only a sharp peak appeared at the Curie temperature on dielectric constant curve. Concurrently, the reductions in dielectric constant and loss tangent became increasingly smaller as the testing frequency was increased from 100 KHz to 1 MHz. For BNT075, its dielectric constants at 100 KHz and 1 MHz were nearly the same, and only a tiny difference between them was observed at temperature near the Curie point and above. So were the loss tangents of this sample. In addition, it can be seen from Fig. 5 that the dielectric constant and loss tangent showed a general decrease with increasing Nd concentration, which could also be attributed to the diminished relaxing polarization in these samples.

3.3.2. Electrical conductivity

Electrical conductivity is one of the most important properties for BIT, high electrical conductivity makes it difficult to polarize the material, and prohibits the material from being used at high temperature. Holly S. Shulman et al. reported that the main conducting mechanism of pure BIT was electronic p-type, and the conductivity of BIT increased with acceptor addition and decreased with donor addition. The alloying of Nb in BIT, which served as a donor, allowed a decrease in conductivity by as much as three orders of magnitude for the sample with a composition of $Bi_4Ti_{2.96}Nb_{0.04}O_{12}$, because of the complete compensation of holes by electrons.[6] In the present study, Nd was chosen to replace part of Bi ions located in the perovskite-like layer of BIT structure. Since Nd ion shows the same valence as Bi, it is neither an acceptor nor a donor dopant for BIT. However, despite that the conductivity of BIT was significantly affected by Nd addition. Fig. 7 shows the temperature response of the electrical conductivity of BIT and BNT075 samples. The BIT sample showed two stages of rapid increase in conductivity with temperature, which started from 80 °C to 300 °C,

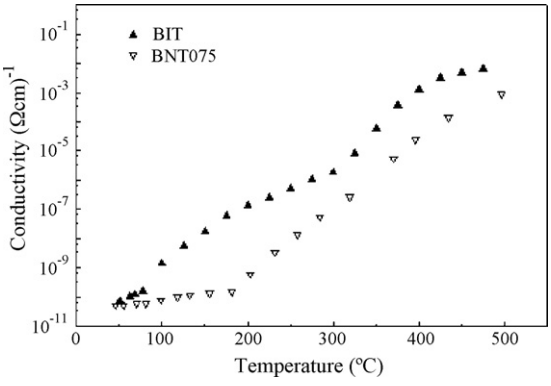

Fig. 7. The temperature response of the electrical conductivity of BIT and BNT075 samples.

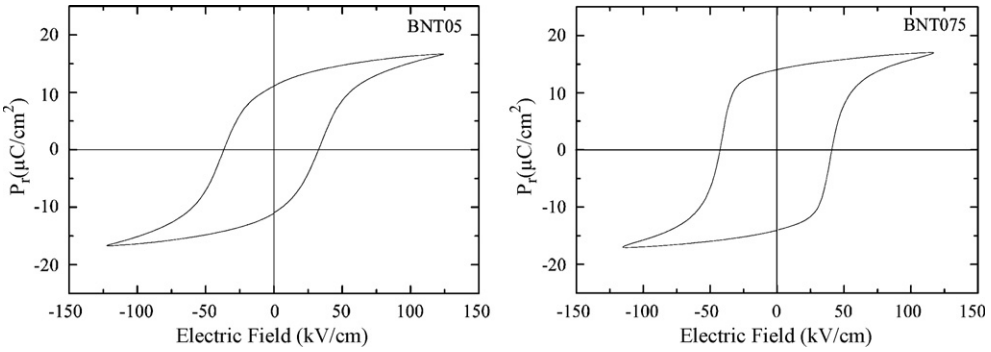

Fig. 8. Ferroelectric hysteresis loops of BNT05 and BNT075 ceramics.

respectively; while the conductivity of BNT075 only showed a single stage of rapid increase with temperature at ~200 °C. This indicated that the electrical conducting mechanism in the present BIT was much more complicated than that in BNT075. Considering the serious volatilization of Bi during sintering of BIT, it is reasonable to assume that electrical conducting associated with vacancies should occur in BIT, aside from the intrinsic hole conducting. Depending on the testing temperature, different conducting mechanism prevailed in the sample, which led to a multistage increase in the electrical conductivity curve.

Furthermore, the conductivity of BNT075 was significantly decreased in comparison with that of BIT. Especially at ~200 °C, the conductivity of BNT075 was nearly four orders of magnitude lower than that of BIT. The decreased conductivity of BNT075 should be mainly ascribed to a decrease in the number of electrical carriers in the sample. As well known, the relationship for electronic conductivity can be expressed as: $\sigma = nze\mu$, where n is the number of charge carriers, ze the charge and μ is the mobility of carriers. Due to the suppression of Bi volatilization by Nd doping, the number of carrier associated with vacancy should be remarkably reduced in BNT075, and this resulted in a significant decrease in the electrical conductivity of the sample.

3.3.3. Ferroelectric property

Fig. 8 shows the ferroelectric hysteresis loops of BNT05 and BNT075. Because of the large loss tangent and high leakage current, hysteresis loops of BIT could not be obtained under present conditions. Neodymium doping led to an improvement in the polarization properties of BIT, which was due to the lowing of electrical conductivity. BNT05 and BNT075 ceramics exhibited well-saturated hysteresis loops. The $2P_r$ and coercive field were 22 $\mu C/cm^2$ and 33 kV/cm for BNT05, and 30 $\mu C/cm^2$ and 40.7 kV/cm for BNT075, respectively. Although these values were a little lower than those of BNT films with preferred grain orientation, they were much higher than those of data reported for pure or lanthanum-doped BIT ceramics.[21–23]

4. Conclusions

Nd-modified BIT (namely BNT) ceramics were fabricated using powders prepared by a hydrolysis method, and systematic studies on the powder characteristics, sintering behavior, microstructure and dielectric properties of the materials were conducted. It was found that:

(1) In Nd-modified BIT (e.g. BNT075), the formation of $Bi_2Ti_2O_7$ intermediate phase during the crystallization process of the powder was suppressed, and the absorption band corresponding to Ti–O bond vibration at 589 cm^{-1} in IR spectra was shifted to higher wave numbers.
(2) The incorporation of Nd in BIT significantly retarded the sintering and grain growth, leading to an increase in the sintering temperature and the formation of fine and homogeneous microstructure.
(3) The Curie temperature of Nd-modified BIT was steadily shifted to lower temperature with increasing Nd concentration. At the same time, the Curie peak on the dielectric curve was greatly depressed.
(4) The incorporation of Nd in BIT suppressed the volatilization of Bi^{3+} during sintering and reduced the bismuth and oxygen vacancy concentrations in the sintered sample. As a result, the dielectric loss and electrical conductivity was significantly reduced, and the polarization properties of the material were greatly improved. A well-saturated and square ferroelectric hysteresis loop was obtained in $Bi_{3.25}Nd_{0.75}Ti_3O_{12}$ sample, which was an interesting result for applications.
(5) With an increase in Nd concentration, the dielectric properties of BNT became much less dependent on temperature and frequency, because of the suppression of relaxing polarization processes in it.

Acknowledgement

This work was supported by the National Natural Science Foundation of China (no. 50472013).

References

1. Park, B. H., Kang, B. S., Bu, S. D., Noh, T. W., Lee, J. and Jo, W., Lanthanum-substituted bismuth titanate for use in non-volatile memories. *Nature*, 1999, **401**, 682–684.
2. Paz de Araujo, C. A., McMillan, L. D., Melnick, B. M., Cuchiargo, J. D. and Scott, J. F., Ferroelectric memories. *Ferroelectrics*, 1990, **104**, 241–256.
3. Fouskova, A. and Cross, L. E., Dielectric properties of bismuth titanate. *J. Appl. Phys.*, 1970, **41**, 2834–2838.

4. Cummins, S. E. and Cross, L. E., Electrical and optical properties of ferroelectric $Bi_4Ti_3O_{12}$ single crystals. *J. Appl. Phys.*, 1968, **39**, 2268–2274.
5. Dorrian, J. F., Newnham, R. E. and Smith, D. K., Crystal structure of $Bi_4Ti_3O_{12}$. *Ferroelectrics*, 1971, **3**, 17–27.
6. Shulman, H. S., Testrof, M., Damjanovic, D. and Setter, N., Microstructure, electrical conductivity, and piezoelectric properties of bismuth titanate. *J. Am. Ceram. Soc.*, 1996, **79**, 3124–3128.
7. Villegas, M., Caballero, A. C., Moure, C., Durán, P. and Fernández, J. F., Factors affecting the electrical conductivity of donor-doped $Bi_4Ti_3O_{12}$ piezoelectric ceramics. *J. Am. Ceram. Soc.*, 1999, **82**, 2411–2416.
8. Kan, Y. M., Jin, X. H., Zhang, G. J., Wang, P. L., Cheng, Y. B. and Yan, D. S., Lanthanum modified bismuth titanate prepared by a hydrolysis method. *J. Mater. Chem.*, 2004, **14**, 3566–3570.
9. Gao, X. S., Xue, J. M. and Wang, J., Ferroelectric behaviors and charge in Nd-doped $Bi_4Ti_3O_{12}$ thin films. *J. Appl. Phys.*, 2005, **97**, 034101.
10. Chon, U. H., Jang, M., Kim, M. K. and Chang, C. H., Layered perovskites with giant spontaneous polarizations for nonvolatile memories. *Phys. Rev. Lett.*, 2002, **89**, 087601.
11. Gang, A., Barber, Z. H., Dawber, M., Scott, J. F., Snedden, A. and Lightfoot, P., Orientation dependence of ferroelectric properties of pulsed-laser-ablated $Bi_{4-x}Nd_xTi_3O_{12}$ films. *Appl. Phys. Lett.*, 2003, **83**, 2414–2416.
12. Kojima, T., Sakai, T., Watanabe, T., Funakubo, H., Saito, K. and Osada, M., Large remanent polarization of $(Bi, Nd)_4Ti_3O_{12}$ epitaxial thin films grown by metalorganic chemical vapor deposition. *Appl. Phys. Lett.*, 2002, **80**, 2746–2748.
13. Johansson, K. E., Palm, T. and Werner, P. E., An automatic microdensitometer for X-ray diffraction photographs. *J. Phys. E: Sci. Instrum.*, 1980, **13**, 1289–1291.
14. Yamaguchi, O., Maruyama, N. and Hirota, K., The formation and characterization of alkoxy-derived $Bi_4Ti_3O_{12}$. *Br. Ceram. Trans. J.*, 1991, **90**, 111–113.
15. Gu, H., Chen, P., Zhou, Y., Zhao, M., Kuang, A. and Li, X., Reactions in preparing $Bi_4Ti_3O_{12}$ ultrafine powders by sol–gel process. *Ferroelectrics*, 1998, **211**, 271–280.
16. Osada, M., Tada, M., Kakihana, M., Watanabe, T. and Funakubo, H., Cation distribution and structure instability in $Bi_{4-x}La_xTi_3O_{12}$. *Jpn. Appl. Phys.*, 2001, **40**, 5572–5575.
17. Jovalekic, C., Atanasoska, L., Petrovic, V. and Ristic, M. M., Sintering and characterization of $Bi_4Ti_3O_{12}$ ceramics. *J. Mater. Sci.*, 1991, **26**, 3553–3564.
18. Xu, T. X., Shen, J. Y., Bo, Z. M., Fang, C. X. and Qu, Y. F., *Electronic Ceramic Materials*. Tianjin University Press, Tianjin, 1993.
19. Shimakawa, Y., Kubo, Y., Nakagawa, Y., Goto, S., Kamiyama, T., Asano, H. and Izumi, F., Crystal structure and ferroelectric properties of $ABi_2Ta_2O_9$ (A=Ca, Sr, and Ba). *Phys. Rev. B*, 2000, **61**, 6559–6564.
20. Luan, W. L., Gao, L. and Guo, J. K., Low temperature sintering of $BaTiO_3$ ceramics. *J. Adv. Mater.*, 1999, **31**, 20–22.
21. Hou, F. M., Shen, R. and Cao, W. W., Ferroelectric properties of neodymium-doped $Bi_4Ti_3O_{12}$ thin films crystallized in different environments. *Thin Solid Films*, 2005, **471**, 35–39.
22. Jovalekic, C. and Stevic, S., A study of ferroelectric properties of $Bi_4Ti_3O_{12}$ ceramics prepared from chemically derived powders. *Ferroelectrics*, 1992, **132**, 185–196.
23. Takenaka, T. and Sakata, K., Electrical properties of grain-oriented ferroelectric ceramics in some lanthanum modified layer-structure oxides. *Ferroelectrics*, 1981, **38**, 769–771.